Supplement to: Elastocapillary Effects Drive Robust Wetting of Cell Aggregates

M. S. Yousafzai[#2,3], V. Yadav[#2,3], S. Amiri[3,4], M.F. Staddon[7], Y. Errami[3,5,6], G. Jaspard[2,3], S. Banerjee[8], M. Murrell*[1,2,3]

[1]Department of Physics, Yale University, 217 Prospect Street, New Haven, Connecticut 06511, USA

[2]Department of Biomedical Engineering, Yale University, 55 Prospect Street, New Haven, Connecticut 06511, USA

[3]Systems Biology Institute, Yale University, 850 West Campus Drive, West Haven, Connecticut 06516, USA

[4]Department of Mechanical Engineering and Material Science, Yale University, 10 Hillhouse Avenue, New Haven, Connecticut 06511, USA

[5]Department of Genetics, Yale School of Medicine, Sterling Hall of Medicine, 333 Cedar Street, New Haven, 06510

[6]Center for Cancer Systems Biology, Yale University, 850 West Campus Drive, West Haven, Connecticut 06516, USA

[7]Department of Physics and Astronomy, Institute for the Physics of Living Systems, University College London, Gower Street, London WC1E 6BT, UK

[8]Department of Physics, Carnegie Mellon University, Pittsburgh, Pennsylvania 15213, USA

*=corresponding author

[#]These authors contributed equally

Supplementary Videos

Supplementary Video 1: Spreading dynamics of an aggregate on a soft substrate

A 3-panel video showing the spreading of an aggregate in DIC and the F-actin fluorescence channel in the first two panels respectively. The third panel shows the magnitude of corresponding traction stresses exerted by cells on the substrate surface. The stiffness of the substrate is 2.8 kPa. Hot and cold colors correspond to high and low traction stresses respectively. On soft substrates, traction stresses are localized immediately under the aggregate. Blue color indicates 0 Pa, whereas red color indicates 100 Pa. The time bar is hour:minutes, and the scale bar is 50 μm.

Supplementary Video 2: Spreading dynamics of an aggregate on a hard substrate

A 3-panel video showing the spreading of an aggregate in DIC and the F-actin fluorescence channel in the first two panels respectively. The third panel shows the magnitude of corresponding traction stresses exerted by cells on the substrate surface. The stiffness of the substrate is 55.0 kPa. Hot and cold colors correspond to high and low traction stresses respectively. On hard substrates traction stresses are localized outside the aggregate. Blue color indicates 0 Pa, whereas red color indicates 100 Pa. The time bar is hour:minutes, and the scale bar is 50 μm.

Supplementary Video 3: Spreading dynamics of a blebbistatin treated aggregate

A 3-panel video showing the spreading of a blebbistatin (50μM) treated aggregate in DIC and the F-actin fluorescence channel in the first two panels respectively. The third panel shows the magnitude of corresponding traction stresses exerted by cells on the substrate surface. The stiffness of the substrate is 8.6 kPa. Hot and cold colors correspond to high and low traction stresses respectively. Imaging actin with 488 nm will inactivate blebbistatin. Blebbistatin treated cells do not exert any traction stress on substrates. Blue color indicates 0 Pa, whereas red color indicates 100 Pa. The time bar is hour:minutes, and the scale bar is 50 μm.

Supplementary Video 4: Indentation on a soft and hard substrate

A 4-panel video showing the z-deformation of the substrate when an aggregate (not shown in the movie) lands on it, as a change in intensity of fluorescently labeled beads embedded in the substrates (top row). The corresponding difference map was obtained by subtracting the intensities of the undeformed substrate from its instantaneous intensity (bottom row). Scale bar is 100 μm.

Supplementary Video 5: Absence of indentation when motor activity is turned off.

A 2-panel video showing the absence of z-deformation on the soft 680 Pa substrate when a blebbistatin-treated aggregate (not shown in the movie) lands on it. No change in intensities is observed in bead intensities or the difference map. The scale bar is 100 μm.

Supplementary Video 6: Internal motion of an aggregate post laser ablation

A 2-panel video showing the internal movement of an aggregate in DIC after laser ablation and the corresponding flow field from particle image velocimetry (PIV). The location of laser ablation is towards the right of the aggregate. The time bar is in seconds. The scale bar is 10 μm.

Table 1: Total number of individual aggregate spreading experiments carried out on two different concentrations of fibronectin on varying substrates stiffnesses (Supplementary Figure 1).

Fibronectin concentration	# of experiments on different Substrate stiffness											Total experiments
	0.68 kPa	2.8 kPa	4 kPa	7 kPa	8.6 kPa	10 kPa	16 kPa	25 kPa	40 kPa	55 kPa	Glass	
0.1 mg/ml	-	15	-	10	20	10	10	-	24	11	-	100
1 mg/ml	26	31	24	-	38		32	15	23	-	21	210

Table 2: Total number of experiments performed to carry out this study. The experiments are reported for each figure.

Figure #	Title	Total # of experiment
Figure 1	Substrate stiffness and aggregate size determine wetting dynamics	121
Figure 2	Traction stresses drive wetting on stiff but not on soft substrates	168
Figure 3	Aggregate adhesion induces solid and fluid-like elasto-capillary effects	132
Figure 4	Capillary forces increase aggregate internal pressure	37
Figure 5	Internal pressure is necessary to drive size-dependent cellular flows on soft substrates	20
Figure 6	Friction differentiates pressure-driven from traction-driven migration	16
	Supplementary Figures Experiments	**103**
	Total # of reported individual experiments	**597**

Table 3: Symbols used in current paper and figures

Appears in	Symbol	Interpretation
Figure 1	$R, (R0)$	Instantaneous radius of aggregate (radius at 90 degree contact angle)
Figure 1	$A, (A0)$	Instantaneous area of aggregate (area at 90 degree contact angle)
Figure 1	E	Stiffness of substrate, in kPa
Figure 2	$\vec{v}$	Speed of aggregate flow (from PIV), in µm/min
Figure 2	$\lvert\vec{\sigma}\rvert$	Magnitude of traction stress on substrate (from TFM), in Pa
Figure 2	σ_r	Radial Traction stress
Figure 3	r	Distance from center of aggregate
Figure 3	$z(r)$	Indentation at a distance r, in µm
Figure 3	l_{max}	Maximum height of meniscus, in µm
Figure 3	z_{max}	Maximum indentation under an aggregate, in µm
Figure 4	γ	Surface Tension of aggregate, in mN/m

Figure 4	γ_s	Aggregate substrate surface tension. In mN/m
Figure 4	P	Pressure (kPa), from indentation
Figure 5	*J1*	Downward flux normal to the substrate
Figure 5	*J2*	Planar outward flux
Figure 5	ρ_s	Cell number density at z=0 µm plane under the aggregate
Figure 5	ρ_0	Density of the aggregate
Figure 5	v_r	Monolayer radial velocity
Figure 5	σ_r	Radial Traction stress
Figure 5	P_m	Pressure (momentum balance)
Figure 5	l	Elasto-capillary length
Figure 6	A_f	Area of focal adhesion in µm^2
Figure 6	q	Scalar nematic order parameter
Figure 6	ς	Effective friction, in Ns/m
Figure 6	v_0	Crawl speed of a cell in simulation
Figure 6	G	Rate of addition of cells to simulation

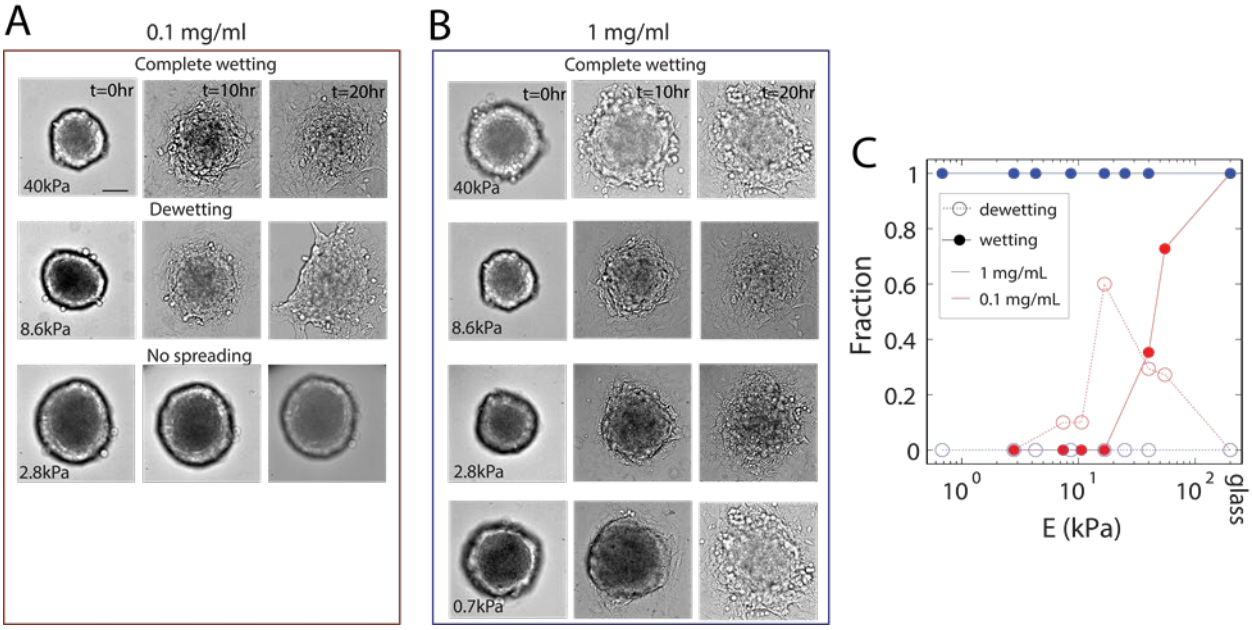

Supplementary Figure 1: Adhesion dependent wetting-dewetting transition: (A) DIC images of substrate dependent (40kPa -2.8kPa) wetting-dewetting transition for substrates with 0.1mg/ml fibronectin. (B) Complete wetting for all substrate stiffnesses for a fibronectin concentration of 1 mg/ml. (C) Fraction of all wetting and de-wetting experiments on varying substrate stiffnesses with 0.1 mg/mL and 1 mg/mL adhesion values. Scale bar is 50 µm.

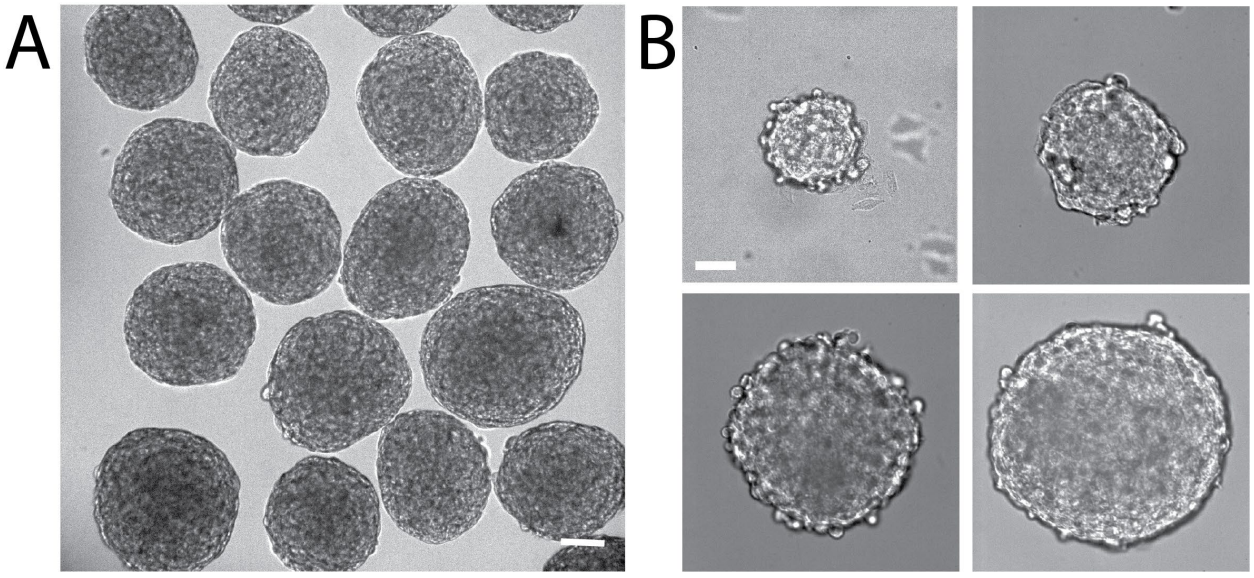

Supplementary Figure 2: **Aggregate preparation with size diversity.** Aggregates of S180 cells were made in a 25 mL flask in a gyratory orbital shaker at 75 rpm at 37 °C for 30-50 hrs. (A) Aggregates in suspension with an average diameter of 150 ± 30 µm are obtained from $2x10^6$ cell in 5ml suspension media. (B) Aggregates of different sizes are obtained by varying the seeding concentration of cells between $1x10^6$ to $3x10^6$. Scale bars are 50 µm.

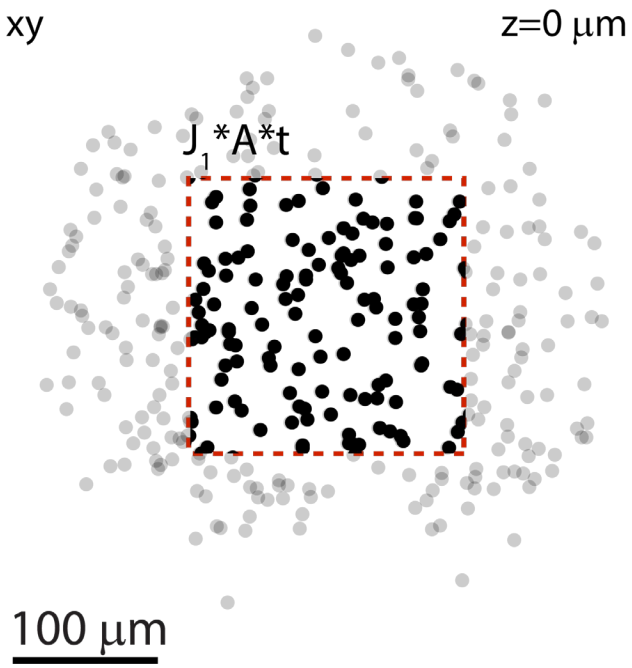

Supplementary Figure 3: Uniform cell efflux from the aggregate cross section (no permeation length). Calculation of the in-plane (z=0 μm) flux of cells to quantify the spreading of an aggregate. Cell flux (J_1) is uniform across the aggregate cross section (red square of area A). Scale bar is 50 μm. Each dot represents a new cell arriving on the substrate within the first 20 hours of spreading. Previous work has suggested this occurs predominantly at the boundary [16].

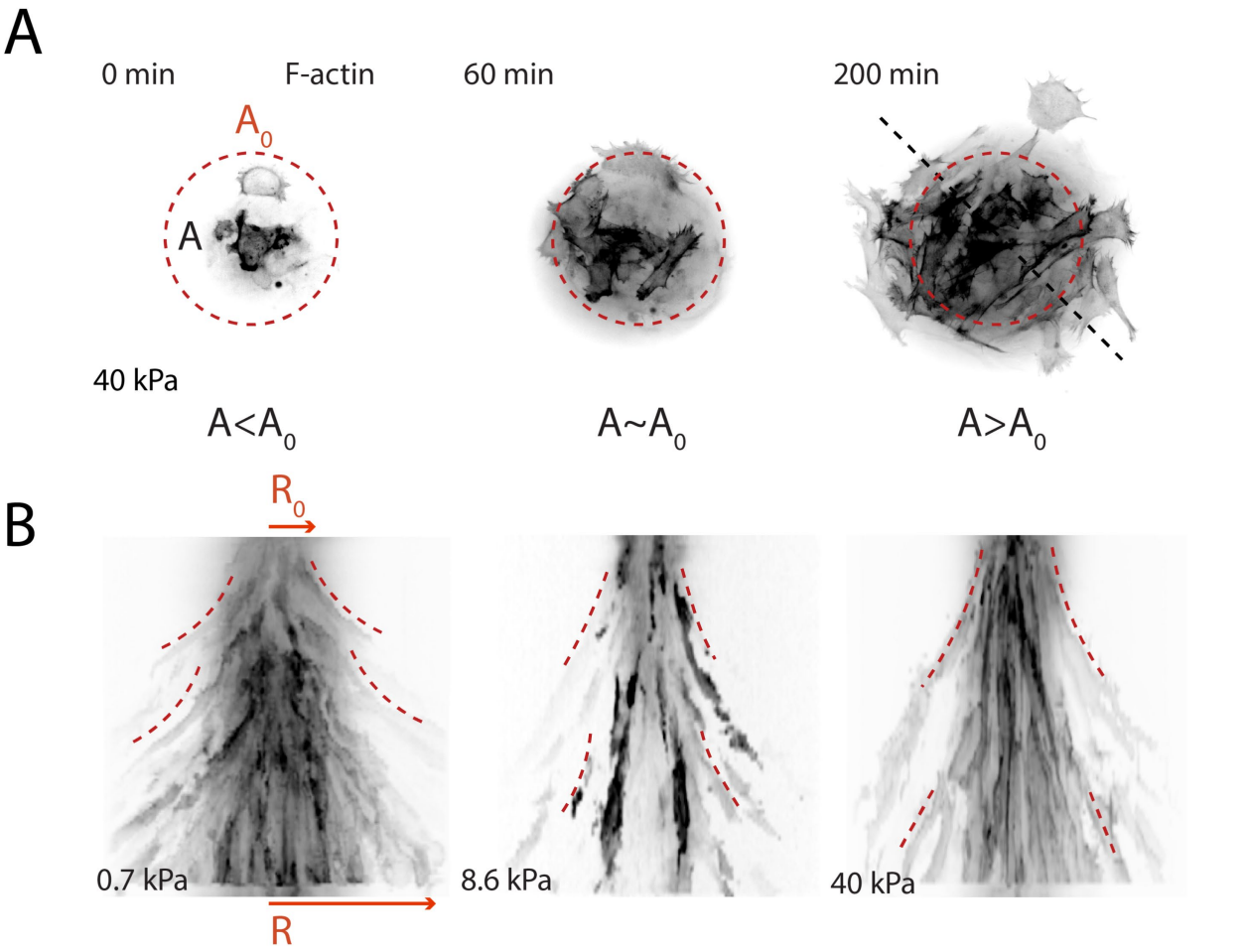

Supplementary Figure 4: Actin flow in spreading aggregates (A) Time-lapse F-actin images of an aggregate on 40kPa substrate. (B) Kymographs of F-actin flow on 0.7 kPa, 8.6kPa and 40kPa substrates with fibronectin concentration 1mg/ml. Expansion of the leading edge on soft substrates (0.7 kPa) are weakly exponential whereas on hard substrates edges show a linear spreading (red dash lines).

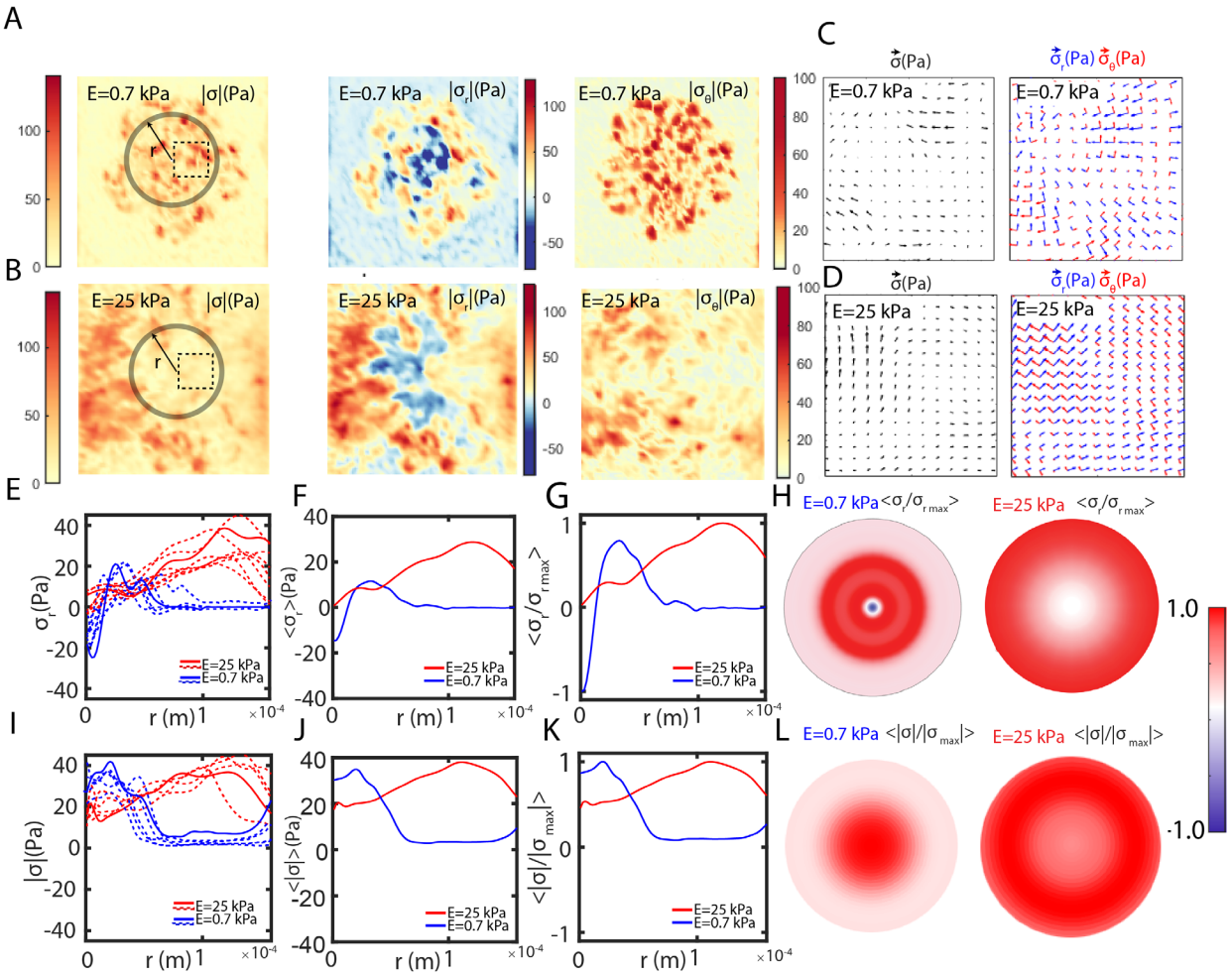

Supplementary Figure 5: Traction force analysis on soft and stiff substrates. Magnitude of the total traction vector $|\sigma|$ (left), the radial component of traction vector $|\sigma_r|$ (middle) and tangential component of traction vector $|\sigma_\theta|$ (right) for soft (A) and stiff (B) substrates. The total traction vector field ($\vec{\sigma}$) (left) and overlays of $\vec{\sigma}_r$ and $\vec{\sigma}_\theta$ for soft (C) and stiff (D) substrates. The vector fields were from the dashed white box region in (A) and (B). Radially averaged σ_r, over concentric circles outwards from center of aggregates (E). Solid line indicates the specific example in (A) and (B) and dashed lines are other samples. Radially averaged σ_r, averaged over N=15 samples (E) and normalized to their maximum stress (G). Visualization of (G) in a polar heatmap after smoothing (H). indicates the specific example in (A) and (B) and dashed lines are other samples. Radially averaged total traction vector σ, over concentric circles outwards from center of aggregates (I). Solid line indicates the specific example in (A) and (B) and dashed lines are other samples. Radially averaged total traction vector σ, averaged over N=12 samples (J) and normalized to their maximum stress (K). Visulaization of (K) in a polar heatmap after smoothing (L).

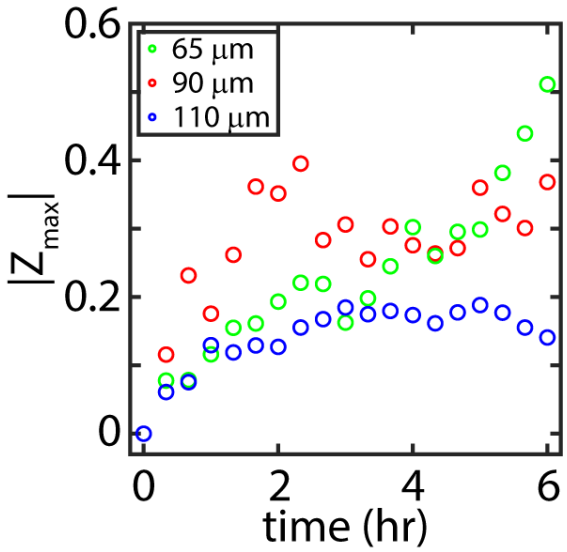

Supplementary Figure 6: Indentation as a function of time: Magnitude of indentation made by aggregates of different sizes as a function of time. Larger aggregates reach a saturating indentation between 2 to 4 hrs, whereas for smaller aggregates this time can be much longer.

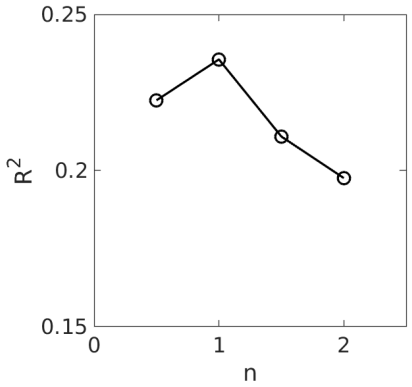

Supplementary Figure 7. Regression shows Pressure varies as $1/R_0$. We fit the data in Fig 3F to functions of the form $z_{max} \sim a/R_0^n$, and quantify the goodness of fit by the R^2 value for different fitting conditions (a is always a free fitting parameter). The goodness of fit (R^2) is maximized when n = 1**.** In addition, if parameters 'a' and 'n' are both free fitting parameters, the best fit occurs for n=0.72 (R^2= 0.25).

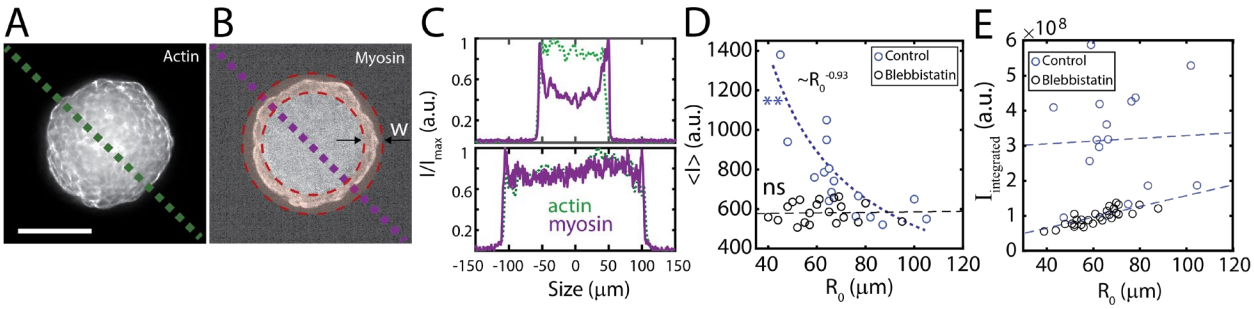

Supplementary Figure 8: Myosin activity is size dependent. Confocal images of F-actin (A) and phospho-myosin light chain 2 (B) at the equatorial plane of a non-adherent aggregate. (C) Normalized myosin intensity (I/I_{max}), as measured across the lines in A and B, is higher at the boundaries as compared to the interior of a R_0=50μm (top) and a R_0=100μm (bottom) aggregate. (D) Average myosin fluorescence intensity on the periphery of width w decays as $1/R_0$ and blebbistatin treatment vanishes size dependence (E) The total peripheral integrated myosin intensity ($I_{integrated}$) for control and blebbistatin treated aggregate. (D, C) Each point represents a single experiment. Scale bar is 50 μm.

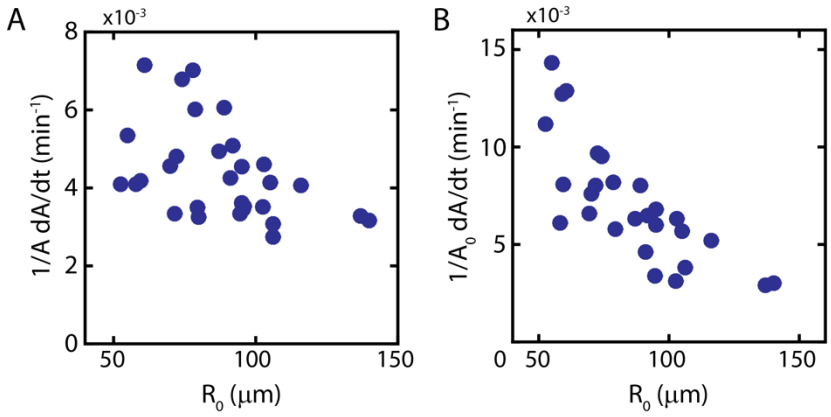

Supplementary Figure 9: Strain rate vs aggregate size: To verify that the decay in strain rate is not a geometric artifact but a true trend, we plot instantaneous strain rate ($\frac{1}{A}\frac{dA}{dt}$) as a function of aggregate size (R_0) (A). (B) This instantaneous strain rate shows a similar decay when strain is calculated with respect to initial aggregate size ($\frac{1}{A_0}\frac{dA}{dt}$).

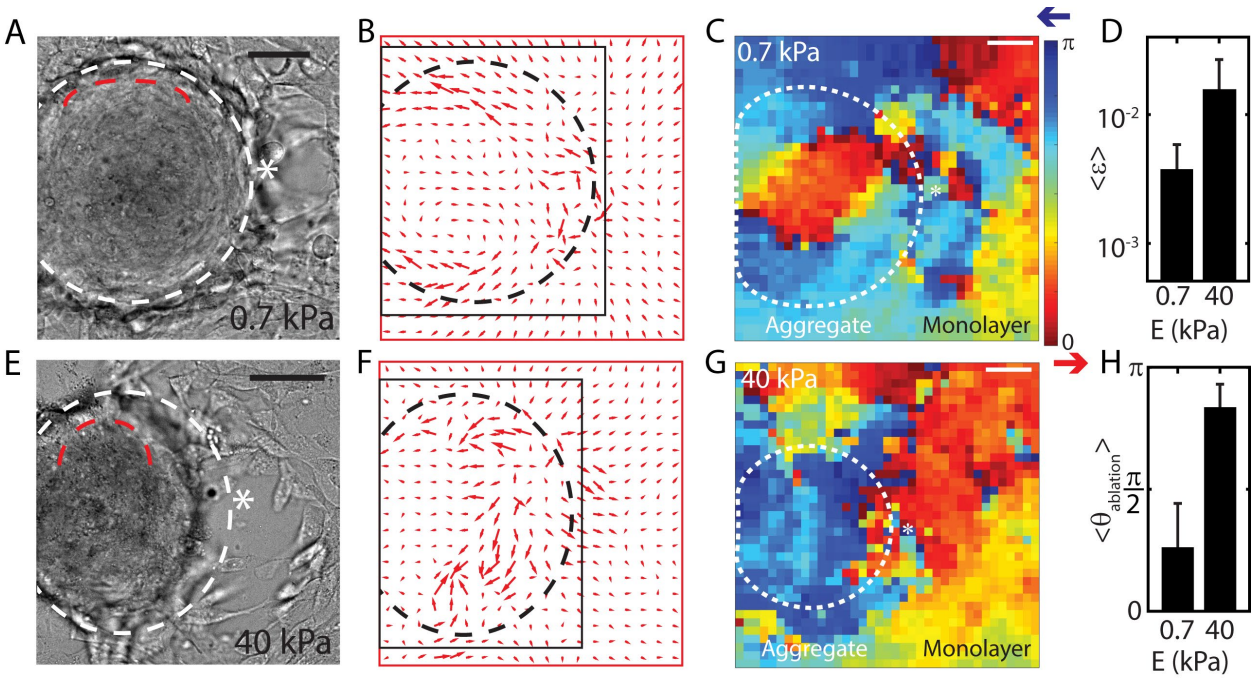

Supplementary Figure 10: Ablation of adherent aggregates show motion due to internal pressure: DIC image of ablated aggregate on a soft, 0.7 kPa substrate (A) and a hard, 40 kPa substrate (E). The white dashed lines mark the original boundary of the aggregates. The '*' symbol marks the location of ablation. (B) and (F) show the post-ablation flow field on soft and hard substrates, respectively. (C) and (G) represent the local orientation field of the flow on soft and hard substrates, respectively. (D) Large mean strains are observed on hard substrates. (H) The mean flow inside aggregate is in the direction of ablation on soft substrate, signifying internal pressure, whereas, on hard substrate, the aggregate retracts, signifying dominant traction.

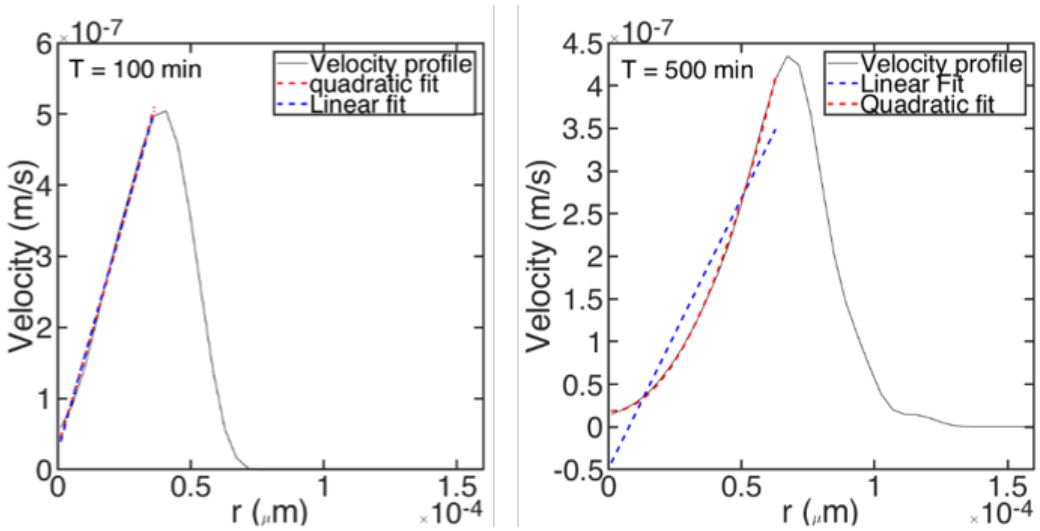

Supplementary Figure 11: Spatial profile of velocity: Spatial profile of velocity scales quadratically at longer times as a function of the radius from the center of monolayer.

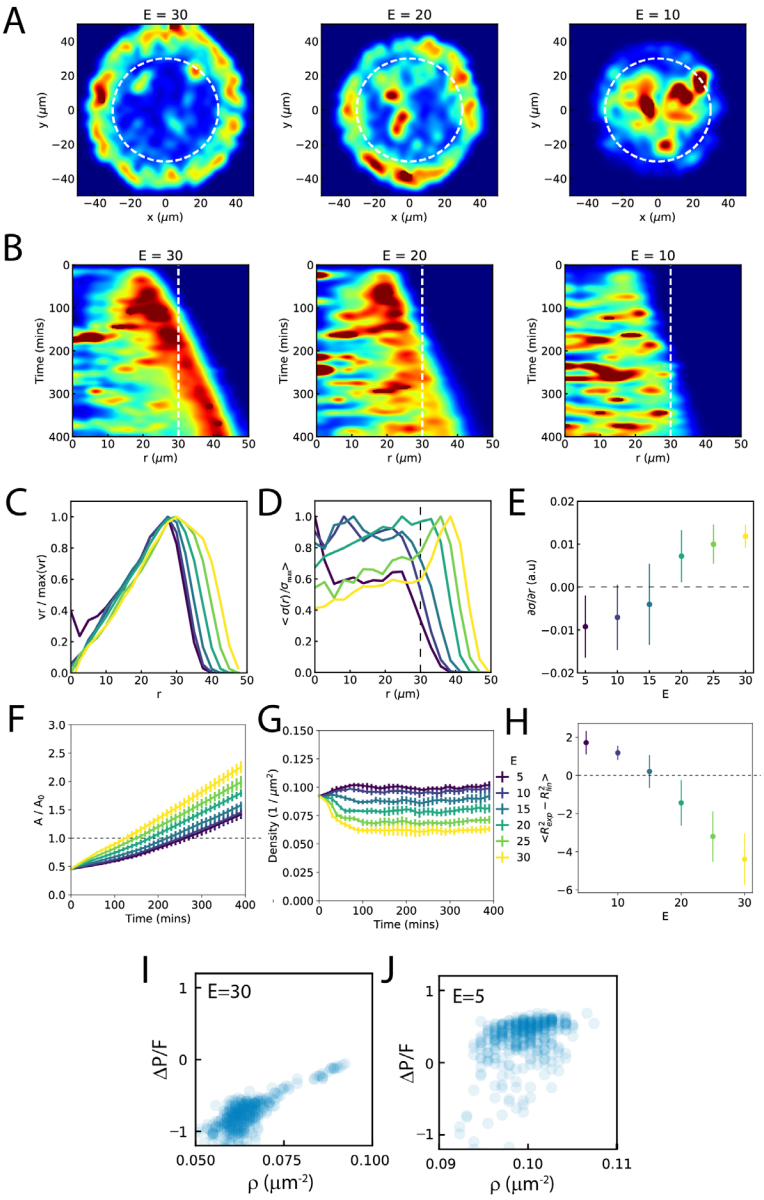

Supplementary Figure 12. Vertex model results. (A) Traction Force Maps (TFM) for E = 30, 20 & 10 (unitless). (B) Kymograph for TFM for E = 30, 20 & 10. (C) Average velocity of cells as a function of distance from the center of the monolayer, *r* (n=10). (D) Average normalized traction stress $(\sigma)/\sigma_{max}$ as a function of distance from the center of the monolayer, *r* (n=10). (E) Traction Stress gradient ($d\sigma/dr$) as a function of substrate stiffness, E (n=10, each). (F) Normalized spreading area as function of time and substrate stiffness (n=10, each). (G) Cell density as function of time and stiffness (n=10, each). (H) Difference in R^2 fitting values as function of stiffness (n=10, each) (I-J) Cell addition accumulates pressure on soft substrates (J), but not (I) on hard substrates (n=10). Error bars are mean +/− standard deviation.

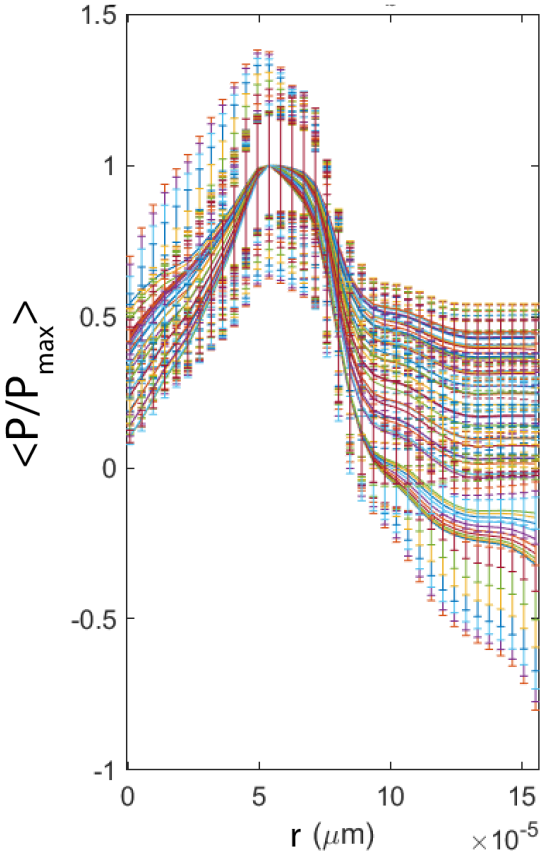

Supplementary Figure 13. Normalized pressure profile showing qualitatively similar profile for viscosities ranging from Pa.s to MPa.s.